

---

---

**Rheology —**

**Part 2:**

**General principles of rotational and  
oscillatory rheometry**

*Rhéologie —*

*Partie 2: Principes généraux de la rhéométrie rotative et oscillatoire*

STANDARDSISO.COM : Click to view the full PDF of ISO 3219-2:2021



STANDARDSISO.COM : Click to view the full PDF of ISO 3219-2:2021



**COPYRIGHT PROTECTED DOCUMENT**

© ISO 2021

All rights reserved. Unless otherwise specified, or required in the context of its implementation, no part of this publication may be reproduced or utilized otherwise in any form or by any means, electronic or mechanical, including photocopying, or posting on the internet or an intranet, without prior written permission. Permission can be requested from either ISO at the address below or ISO's member body in the country of the requester.

ISO copyright office  
CP 401 • Ch. de Blandonnet 8  
CH-1214 Vernier, Geneva  
Phone: +41 22 749 01 11  
Email: [copyright@iso.org](mailto:copyright@iso.org)  
Website: [www.iso.org](http://www.iso.org)

Published in Switzerland

# Contents

	Page
Foreword .....	iv
<b>1 Scope</b> .....	<b>1</b>
<b>2 Normative references</b> .....	<b>1</b>
<b>3 Terms and definitions</b> .....	<b>1</b>
<b>4 Symbols</b> .....	<b>3</b>
<b>5 Measuring principles</b> .....	<b>4</b>
5.1 General .....	4
5.2 Rotational rheometry .....	5
5.3 Oscillatory rheometry .....	6
<b>6 Measuring assembly</b> .....	<b>8</b>
6.1 General .....	8
6.2 Temperature control systems .....	9
6.3 Measuring geometries .....	9
6.3.1 General .....	9
6.3.2 Absolute measuring geometries .....	10
6.3.3 Relative measuring geometries .....	20
6.4 Selected optional accessories .....	24
6.4.1 Cover with or without solvent trap .....	24
6.4.2 Passive and active thermal covers .....	25
6.4.3 Stepped plates .....	26
<b>Annex A (informative) Information on rheometry and flow field patterns</b> .....	<b>27</b>
<b>Bibliography</b> .....	<b>45</b>

STANDARDSISO.COM : Click to view the full PDF of ISO 3219-2:2021

## Foreword

ISO (the International Organization for Standardization) is a worldwide federation of national standards bodies (ISO member bodies). The work of preparing International Standards is normally carried out through ISO technical committees. Each member body interested in a subject for which a technical committee has been established has the right to be represented on that committee. International organizations, governmental and non-governmental, in liaison with ISO, also take part in the work. ISO collaborates closely with the International Electrotechnical Commission (IEC) on all matters of electrotechnical standardization.

The procedures used to develop this document and those intended for its further maintenance are described in the ISO/IEC Directives, Part 1. In particular, the different approval criteria needed for the different types of ISO documents should be noted. This document was drafted in accordance with the editorial rules of the ISO/IEC Directives, Part 2 (see [www.iso.org/directives](http://www.iso.org/directives)).

Attention is drawn to the possibility that some of the elements of this document may be the subject of patent rights. ISO shall not be held responsible for identifying any or all such patent rights. Details of any patent rights identified during the development of the document will be in the Introduction and/or on the ISO list of patent declarations received (see [www.iso.org/patents](http://www.iso.org/patents)).

Any trade name used in this document is information given for the convenience of users and does not constitute an endorsement.

For an explanation of the voluntary nature of standards, the meaning of ISO specific terms and expressions related to conformity assessment, as well as information about ISO's adherence to the World Trade Organization (WTO) principles in the Technical Barriers to Trade (TBT), see [www.iso.org/iso/foreword.html](http://www.iso.org/iso/foreword.html).

This document was prepared by Technical Committee ISO/TC 35, *Paints and varnishes*, Subcommittee SC 9, *General test methods for paints and varnishes*, in collaboration with the European Committee for Standardization (CEN) Technical Committee CEN/TC 139, *Paints and varnishes*, in accordance with the Agreement on technical cooperation between ISO and CEN (Vienna Agreement), and in cooperation with ISO/TC 61, *Plastics, SC 5, Physical-chemical properties*.

This document cancels and replaces ISO 3219:1993, which have been technically revised. The main changes compared to the previous editions are as follows:

- plate-plate measuring geometry has been added;
- relative measuring geometries have been added;
- oscillatory rheometry has been added.

A list of all parts in the ISO 3219 series can be found on the ISO website.

Any feedback or questions on this document should be directed to the user's national standards body. A complete listing of these bodies can be found at [www.iso.org/members.html](http://www.iso.org/members.html).

# Rheology —

## Part 2: General principles of rotational and oscillatory rheometry

### 1 Scope

This document specifies the general principles of rotational and oscillatory rheometry.

Detailed information is presented in [Annex A](#). Further background information is covered in subsequent parts of the ISO 3219 series, which are currently in preparation.

### 2 Normative references

The following documents are referred to in the text in such a way that some or all of their content constitutes requirements of this document. For dated references, only the edition cited applies. For undated references, the latest edition of the referenced document (including any amendments) applies.

ISO 3219-1, *Rheology — Part 1: General terms and definitions for rotational and oscillatory rheometry*

### 3 Terms and definitions

For the purposes of this document, the terms and definitions given in ISO 3219-1 and the following apply.

ISO and IEC maintain terminological databases for use in standardization at the following addresses:

- ISO Online browsing platform: available at <https://www.iso.org/obp>
- IEC Electropedia: available at <http://www.electropedia.org/>

#### 3.1

##### measuring gap

space between the boundary surfaces of the measuring geometry

#### 3.2

##### gap width

$h$

$H_{cc}$

$H_{cp}$

distance between the boundary surfaces of the measuring geometry

Note 1 to entry: The symbol  $h$  refers to a gap width that can be varied (e.g. plate-plate measuring geometry); the symbol  $H$  refers to a gap width which is not variable and which is defined by the relevant measuring geometry.  $H_{cc}$  is the gap width of the coaxial-cylinders geometry.  $H_{cp}$  is the gap width of the cone-plate geometry.

Note 2 to entry: The distance between the boundary surfaces is given by the difference in the radii (coaxial cylinders), the cone angle (cone-plate) or the distance between the two plates.

Note 3 to entry: In cone-plate measuring geometries, the gap width varies as a function of the radius across the measuring geometry. The value  $H_{cp}$  is the distance between the flattened cone tip and the plate.

**3.3**  
**flow field coefficient**  
**geometric factor**

$k$   
quotient of the shear stress factor (3.9)  $k_\tau$  and the strain factor (3.8)  $k_\gamma$

Note 1 to entry: The flow field coefficient  $k$  relates the angular velocity  $\Omega$  and torque  $M$  to the shear viscosity  $\eta$  of the fluid as given by the following formula:

$$\eta = k \cdot \frac{M}{\Omega}$$

The flow field coefficient  $k$  is expressed in radians per cubic metre ( $\text{rad}\cdot\text{m}^{-3}$ ). It can be calculated from the shape and dimensions of an *absolute measuring geometry* (3.7).

**3.4**  
**no-slip condition**

presence of a relative velocity of zero between a boundary surface and the immediately adjacent fluid layer

**3.5**  
**wall slip**

presence of a non-zero relative velocity between a boundary surface and the immediately adjacent fluid layer

**3.6**  
**relative measuring geometry**

measuring geometry for which the flow profile and thus the rheological parameters cannot be calculated

Note 1 to entry: For relative measuring geometries, the viscosity shall not be given in pascal multiplied by seconds (Pa·s) except in the case of plate-plate measuring geometries if the correction referred to in 6.3.3.1.2 is used.

**3.7**  
**absolute measuring geometry**

measuring geometry for which the flow profile and thus the rheological parameters can be calculated exactly for the entire sample, regardless of its flow properties

**3.8**  
**strain factor**

$k_\gamma$   
proportionality factor between the angular deflection  $\varphi$  and shear strain  $\gamma$  for *absolute measuring geometries* (3.7)

Note 1 to entry: The absolute value of the strain factor corresponds to the absolute value of the shear rate factor. The latter is the proportionality factor between the shear rate  $\dot{\gamma}$  and the angular velocity  $\Omega$ .

Note 2 to entry: This factor is called the shear rate factor in the rotation test and the strain factor in the oscillatory test.

Note 3 to entry: The strain factor  $k_\gamma$  has units of reciprocal radians ( $\text{rad}^{-1}$ ).

**3.9**  
**shear stress factor**

$k_\tau$   
proportionality factor between the torque  $M$  and the shear stress  $\tau$  for *absolute measuring geometries* (3.7)

Note 1 to entry: The shear stress factor  $k_\tau$  has units of reciprocal cubic metres ( $\text{m}^{-3}$ ).

## 4 Symbols

Table 1 — Symbols and units

Meaning	Symbol	Unit
Absolute value of the complex shear modulus	$ G^* $	Pa
Absolute value of the complex viscosity	$ \eta^* $	Pa·s
Acceleration of the angular deflection	$\ddot{\varphi}$	rad·s <sup>-2</sup>
Amplitude of the angular deflection of the motor	$\varphi_{M,0}^*$	rad
Amplitude of angular deflection of torque transducer	$\varphi_{D,0}^*$	rad
Amplitude of the angular deflection	$\varphi_0$	rad
Amplitude of the angular velocity	$\dot{\varphi}_0$	rad·s <sup>-1</sup>
Amplitude of the shear rate	$\dot{\gamma}_0$	s <sup>-1</sup>
Amplitude of the shear strain	$\gamma_0$	1
Amplitude of the shear stress	$\tau_0$	Pa
Amplitude of the torque	$M_0$	N·m
Angular acceleration of motor	$\ddot{\varphi}_M^*$	rad·s <sup>-2</sup>
Angular acceleration of torque transducer	$\ddot{\varphi}_D^*$	rad·s <sup>-2</sup>
Angular deflection	$\varphi$	rad
Angular deflection of motor	$\varphi_M^*$	rad
Angular deflection of sample	$\varphi_P^*$	rad
Angular deflection of torque transducer	$\varphi_D^*$	rad
Angular frequency	$\omega$	rad·s <sup>-1</sup> or s <sup>-1</sup>
Angular velocity across the measuring gap	$\omega(r)$	rad·s <sup>-1</sup>
Angular velocity (presented in brackets: as the time derivative of the angular deflection)	$\Omega, (\dot{\varphi})$	rad·s <sup>-1</sup>
Angular velocity of motor	$\dot{\varphi}_M^*$	rad·s <sup>-1</sup>
Angular velocity of torque transducer	$\dot{\varphi}_D^*$	rad·s <sup>-1</sup>
Coefficient of bearing friction	$D_L$	N·m·s
Coefficient of friction	$D$	N·m·s
Complex angular deflection	$\varphi^*$	rad
Complex shear modulus	$G^*$	Pa
Complex torque	$M^*$	N·m
Complex viscosity	$\eta^*$	Pa·s
Cone angle	$\alpha$	° or rad
Deflection path	$s$	m
Drive loss factor	$\tan \zeta$	1
Drive phase angle	$\zeta$	rad
Face factor	$c_L$	1
Flow field coefficient, geometric factor	$k$	rad·m <sup>-3</sup>
Frequency	$f$	Hz
NOTE The parameters marked with an * refer to complex-valued parameters whose real part is denoted by ' and imaginary part by ''.		

Table 1 (continued)

Meaning	Symbol	Unit
Gap width	$h$	m
Gap width defined by the coaxial cylinders geometry	$H_{cc}$	m
Gap width defined by the cone-plate geometry	$H_{cp}$	m
Geometry compliance	$C_G$	$\text{rad}\cdot(\text{N}\cdot\text{m})^{-1}$
Imaginary part of the complex viscosity	$\eta''$	$\text{Pa}\cdot\text{s}$
Imaginary unit	$i$	1
Loss angle, phase angle	$\delta$	rad
Loss factor	$\tan\delta$	1
Moment of inertia	$I$	$\text{N}\cdot\text{m}\cdot\text{s}^2$
Real part of the complex viscosity	$\eta'$	$\text{Pa}\cdot\text{s}$
Rotational speed	$n$	$\text{s}^{-1}$ or $\text{min}^{-1}$
Sample torque	$M_p^*$	$\text{N}\cdot\text{m}$
Shear force	$F$	N
Shear loss modulus, viscous shear modulus	$G''$	Pa
Shear modulus	$G$	Pa
Shear plane	$A$	$\text{m}^2$
Shear rate factor	$k_{\dot{\gamma}}$	$\text{rad}^{-1}$
Shear rate, shear deformation rate	$\dot{\gamma}$	$\text{s}^{-1}$
Shear storage modulus, elastic shear modulus	$G'$	Pa
Shear strain, shear deformation	$\gamma$	1 or %
Shear stress	$\tau$	Pa
Shear stress factor	$k_\tau$	$\text{m}^{-3}$
Shear viscosity	$\eta$	$\text{Pa}\cdot\text{s}$
Strain factor	$k_\gamma$	$\text{rad}^{-1}$
Temperature	$T$	$^\circ\text{C}$ or K
Time	$t$	s
Torque	$M$	$\text{N}\cdot\text{m}$
Torque applied by motor	$M_M^*$	$\text{N}\cdot\text{m}$
Torque caused by bearing friction	$M_L^*$	$\text{N}\cdot\text{m}$
Torque caused by transducer inertia	$M_I^*$	$\text{N}\cdot\text{m}$
Torque measured by transducer	$M_m^*$	$\text{N}\cdot\text{m}$
Torsional compliance of the measurement system	$C$	$\text{rad}\cdot(\text{N}\cdot\text{m})^{-1}$
Velocity	$v$	$\text{m}\cdot\text{s}^{-1}$

NOTE The parameters marked with an \* refer to complex-valued parameters whose real part is denoted by ' and imaginary part by ''.

## 5 Measuring principles

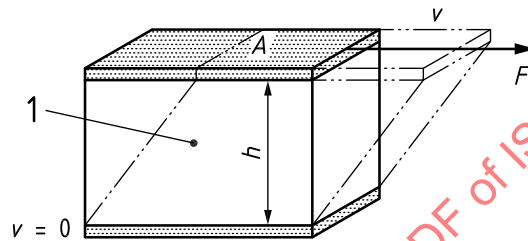
### 5.1 General

There are rotational tests, oscillatory tests and various step tests. The different tests can be combined with one another.

These can be carried out using various measuring types: controlled deformation (CD), controlled rate (CR) or controlled stress (CS).

## 5.2 Rotational rheometry

In the basic rotational test, the sample is subjected to constant or variable loading in one direction. The shear viscosity  $\eta$  is calculated from the measured data. The corresponding mechanical input and response parameters are listed in [Tables A.1](#) and [A.3](#). The basic parameters of the test can be represented schematically in terms of the two-plates model. An infinitesimal element of the measuring geometry is considered in this subclause (see [Figure 1](#)). The two-plates model consists of two parallel plates, each with a surface area  $A$  and with a gap width  $h$ , between which the sample is located. The velocity of the lower plate is zero ( $v = 0$ ). The upper plate is moved by a defined shear force  $F$ , which results in a velocity  $v$ . It is assumed that the sample between the plates consists of layers that move at different velocities of between  $v = 0$  and  $v$ .



### Key

- 1 sample
- $v$  velocity
- $A$  shear plane
- $h$  gap width
- $F$  shear force

**Figure 1 — Two-plate model with a simplified schematic representation of the basic parameters of a rotational test**

With this model, the following parameters are calculated using [Formulae \(1\)](#) to [\(3\)](#):

$$\tau = \frac{F}{A} \quad (1)$$

where

- $\tau$  is the shear stress, in pascals;
- $F$  is the shear force, in newtons;
- $A$  is the shear plane, in square metres.

$$\dot{\gamma} = \frac{v}{h} \quad (2)$$

where

- $\dot{\gamma}$  is the shear rate, in reciprocal seconds;
- $v$  is the velocity, in metres per second;
- $h$  is the gap width, in metres.

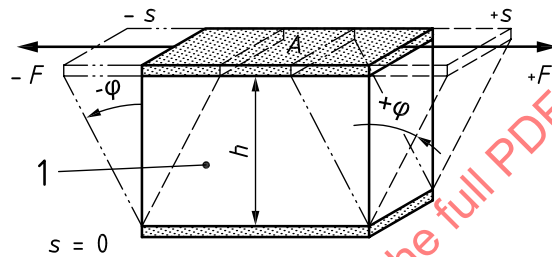
Based on the Newtonian law of viscosity, the shear viscosity can be calculated using [Formula \(3\)](#):

$$\eta = \frac{\tau}{\dot{\gamma}} \tag{3}$$

where  $\eta$  is the shear viscosity, in pascal multiplied by seconds.

### 5.3 Oscillatory rheometry

In the basic oscillatory test, the sample is stimulated with an angular deflection or torque amplitude at a given oscillation frequency. The resulting response oscillates with the same frequency and is characterized by an amplitude and phase shift. The corresponding mechanical input and response parameters are listed in [Tables A.2](#) and [A.3](#). Parameters such as the shear storage modulus  $G'$  (elastic shear modulus), the shear loss modulus  $G''$  (viscous shear modulus), the absolute value of the complex viscosity  $|\eta^*|$  and the loss factor  $\tan \delta$  can be calculated from the measured data in order to characterize the viscoelastic behaviour. The mathematical principles are presented in [A.3](#). The basic parameter of the test can be represented schematically in terms of the two-plates model (see [Figure 2](#)).



**Key**

- 1 sample
- s deflection path
- $\varphi$  deflection angle
- A shear plane
- h gap width
- F shear force

**Figure 2 — Two-plate model with a simplified schematic representation of the basic parameters of an oscillatory test**

With this model, the following parameters can be calculated using [Formula \(4\)](#):

$$\gamma = \frac{s}{h} \tag{4}$$

where

- $\gamma$  is the shear strain, dimensionless;
- s is the deflection path, in metres;
- h is the gap width, in metres.

In the oscillatory test, the shear strain  $\gamma$  varies sinusoidally as a function of time  $t$ , see [Figure 3](#). The associated shear stress  $\tau$  is shifted within the viscoelastic range by the loss angle  $\delta$  at the same angular frequency  $\omega$ . [Formulae \(5\)](#) and [\(6\)](#) apply:

$$\gamma(t) = \gamma_0 \sin(\omega t) \quad (5)$$

where

$\gamma_0$  is the amplitude of the shear strain, dimensionless;

$\omega$  is the angular frequency, in radians per second;

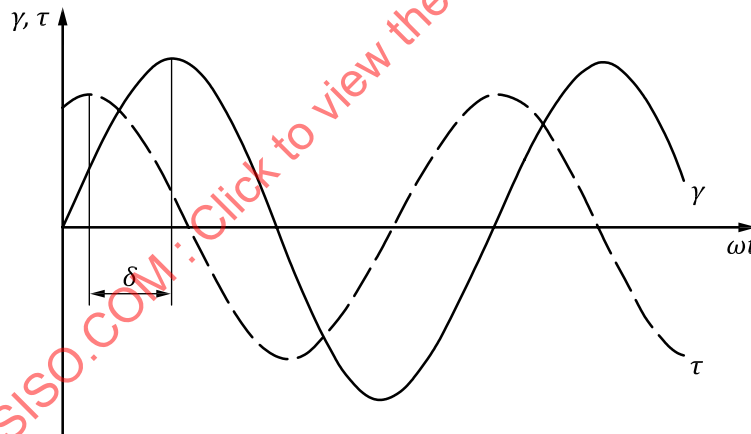
$t$  is the time, in seconds.

$$\tau(t) = \tau_0 \sin(\omega t + \delta) \quad (6)$$

where

$\tau_0$  is the amplitude of the shear stress, in pascals;

$\delta$  is the loss angle, in radians.



#### Key

- $\gamma$  shear strain
- $\tau$  shear stress
- $\omega$  angular frequency
- $t$  time
- $\delta$  loss angle

**Figure 3 — Schematic representation of the shear strain and shear stress functions for an oscillatory test**

NOTE Degrees ( $^{\circ}$ ) are commonly used in practice as the unit for the loss angle  $\delta$ . The following conversion applies:  $2\pi \text{ rad} = 360^{\circ}$ .

In the case of ideal elastic behaviour (in accordance with Hooke's law), the loss angle has a value of  $\delta = 0^{\circ}$ , i.e. the shear strain and shear stress are always in phase. In the case of ideal viscous behaviour (in accordance with Newton's law), the loss angle has a value of  $\delta = \pi/2 = 90^{\circ}$ , i.e. the shear stress curve is  $90^{\circ}$  ahead of the shear strain curve.

Using Hooke's elasticity law, the complex shear modulus  $G^*$  and its absolute value  $|G^*|$  can be calculated using [Formulae \(7\)](#) and [\(8\)](#):

$$G^* = \frac{\tau(t)}{\gamma(t)} \quad (7)$$

$$|G^*| = \sqrt{G'^2 + G''^2} \quad (8)$$

where

$G^*$  is the complex shear modulus, in pascals;

$G'$  is the shear storage modulus, in pascals;

$G''$  is the shear loss modulus, in pascals;

$G^*$  describes the overall viscoelastic behaviour.

This can be separated into an elastic component  $G'$  (shear storage modulus) and a viscous component  $G''$  (shear loss modulus) using [Formulae \(9\)](#) and [\(10\)](#).

$$G' = \frac{\tau_0}{\gamma_0} \cos \delta \quad (9)$$

$$G'' = \frac{\tau_0}{\gamma_0} \sin \delta \quad (10)$$

The quotient of the shear loss modulus  $G''$  and shear storage modulus  $G'$  is the dimensionless loss factor  $\tan \delta$ , see [Formula \(11\)](#):

$$\tan \delta = \frac{G''}{G'} \quad (11)$$

The ratio of the absolute value of the complex shear modulus  $G^*$  and the angular frequency  $\omega$  is the absolute value of the complex viscosity  $\eta^*$ , see [Formula \(12\)](#):

$$|\eta^*| = \frac{|G^*|}{\omega} \quad (12)$$

where  $|\eta^*|$  is the absolute value of the complex viscosity, in pascal multiplied by seconds.

## 6 Measuring assembly

### 6.1 General

The rheological properties are investigated using a measuring system consisting of a measuring device (viscometer or rheometer) and a measuring geometry (e.g. cone-plate).

The viscometer can only measure the viscosity in rotation (viscometry). This means that the viscosity function of the sample can be determined as a function of the parameters of time, temperature, shear rate, shear stress and others such as pressure.

With a rheometer, it is possible to carry out all basic tests in rotation and oscillation (rheometry). Alongside the viscosity function, the viscoelastic properties can be determined, e.g. shear storage modulus and shear loss modulus.

A measuring assembly, consisting of a measuring device, a measuring geometry and optional accessories, is shown in Figure 4. The measuring device and individual components, such as the temperature control system, can be computer-controlled.

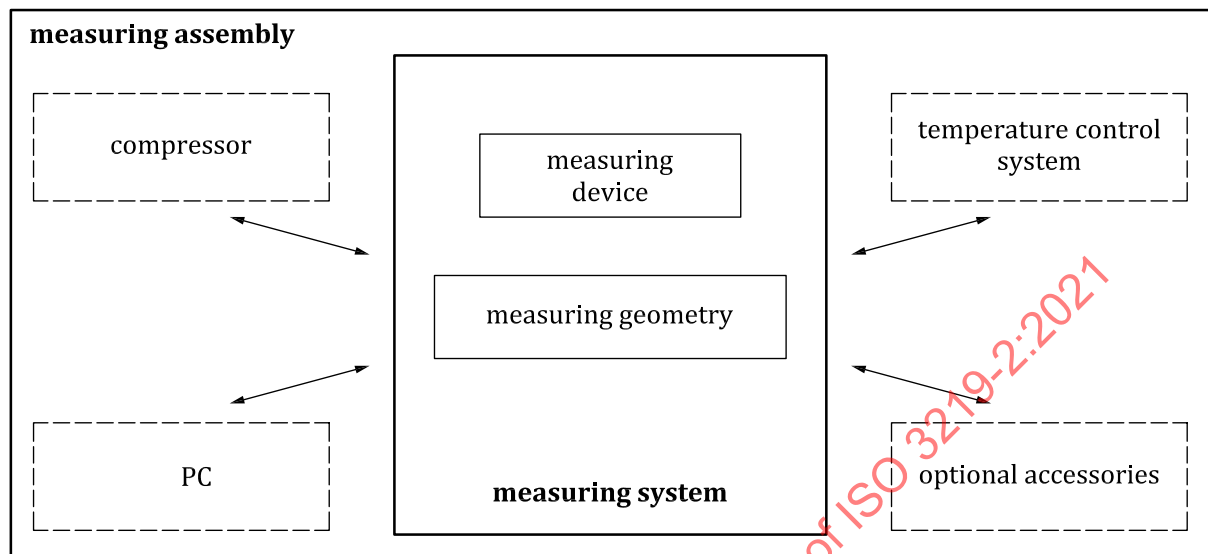


Figure 4 — Example of a measuring assembly

The sample to be investigated is located in a measuring gap where a defined flow profile is generated in the sample. A necessary prerequisite for this is a sufficiently small gap width. When viscometers or rheometers are used, they shall be able to impose or detect torque or rotational speed/angular deflection. The imposed parameter shall be adjustable both in time-dependent and time-independent manners.

For viscometric measurements, all viscometers are principally suitable, regardless of how the drive and/or detection unit are supported. For measurements in oscillation, rheometers shall be used that have the lowest possible internal friction in the drive or detection unit.

To cover the broadest possible range of applications, the viscometer or rheometer shall be able to work with different measuring geometries. The range of the torques or angular deflections, that result and the measuring range that can be achieved, depend on the measuring system. The type of measuring device and measuring geometry to be selected depends on the sample.

## 6.2 Temperature control systems

A temperature control system consists of one or more temperature control components for heating and/or cooling, including the required media (e.g. air, water, liquid nitrogen) and the necessary connections (e.g. hoses and insulation for these hoses).

The rheological properties of the sample are temperature-dependent. As a result, measures such as controlling of the sample temperature and its measurement with one or more temperature sensors in the immediate vicinity of the sample are required.

The temperature of the sample shall be kept constant as a function of time during the measurement period.

## 6.3 Measuring geometries

### 6.3.1 General

A measuring geometry consists of two parts that form a sample chamber where the sample is located. A measuring geometry consists of a rotor and a stator or of two rotors.

The measuring geometry shall be selected in such a way that its dimensions are suitable for the expected viscosity range and viscoelastic properties of the sample. With regard to its gap width, the measuring geometry shall also be selected in such a way that possible heterogeneities in the sample (e.g. particles, droplets, air bubbles) are considered. The magnitude of these heterogeneities is to be determined in advance using suitable methods (e.g. microscopy, laser diffraction, sieving or determination of fineness of grind).

The absolute and relative measuring geometries of a rotational viscometer or rheometer are described below.

Coaxial cylinders, double-gap and cone-plate measuring geometries are absolute measuring geometries. All the others are relative measuring geometries.

In the case of an absolute measuring geometry, the flow profile within the complete sample can be calculated exactly, regardless of its flow properties. This applies under the condition of laminar flow, and without slip (wall slip or slip between flow layers).

In the case of relative measuring geometries apart from plate-plate measuring geometries, calculation of the flow profile is only possible if the flow properties of the sample are known.

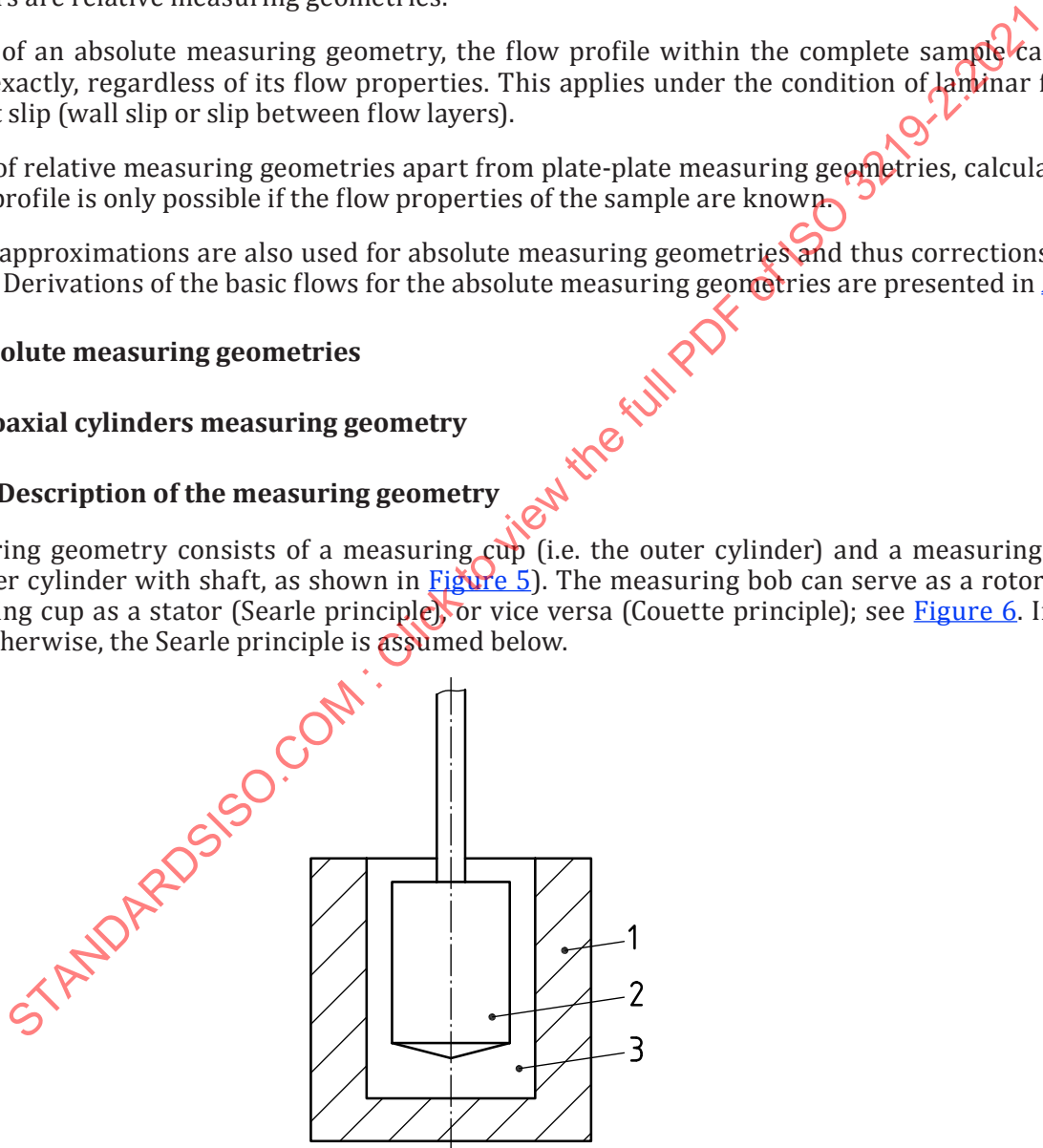
In practice, approximations are also used for absolute measuring geometries and thus corrections are carried out. Derivations of the basic flows for the absolute measuring geometries are presented in [A.2](#).

### 6.3.2 Absolute measuring geometries

#### 6.3.2.1 Coaxial cylinders measuring geometry

##### 6.3.2.1.1 Description of the measuring geometry

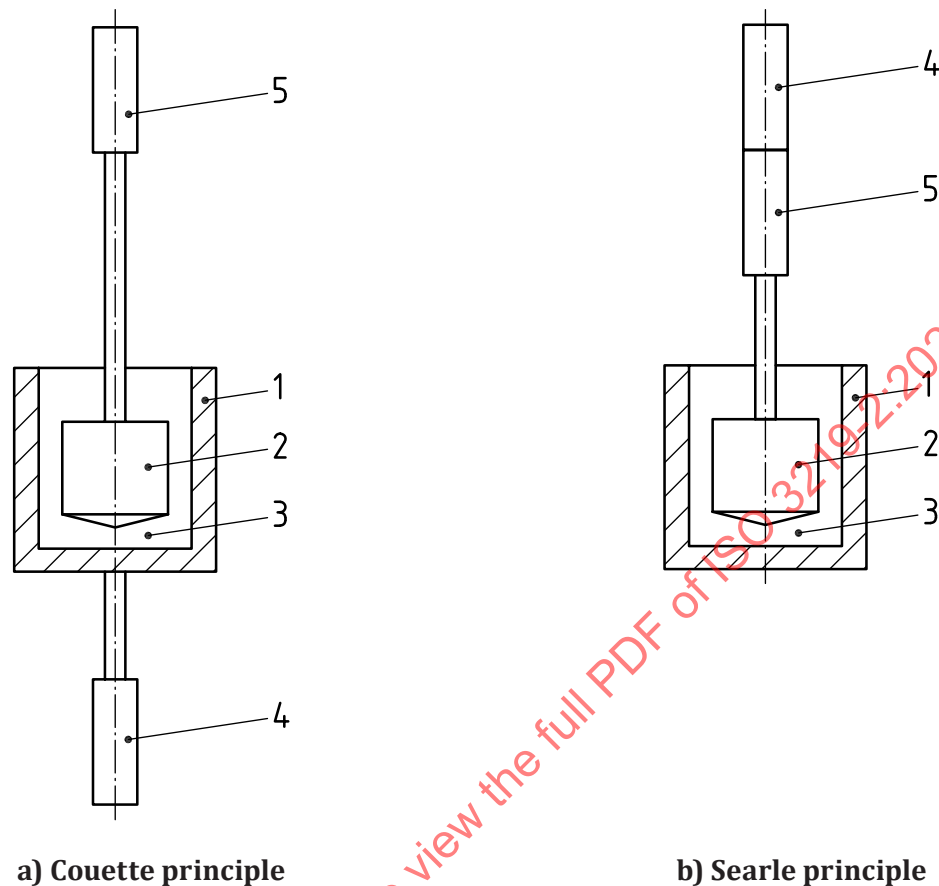
The measuring geometry consists of a measuring cup (i.e. the outer cylinder) and a measuring bob (i.e. the inner cylinder with shaft, as shown in [Figure 5](#)). The measuring bob can serve as a rotor and the measuring cup as a stator (Searle principle), or vice versa (Couette principle); see [Figure 6](#). If not indicated otherwise, the Searle principle is assumed below.



**Key**

- 1 measuring cup (outer cylinder)
- 2 measuring bob (inner cylinder)
- 3 sample chamber

**Figure 5 — Schematic drawing of a coaxial cylinders measuring geometry**

**Key**

- 1 measuring cup (outer cylinder)
- 2 measuring bob (inner cylinder)
- 3 sample chamber
- 4 drive
- 5 measuring sensor

**Figure 6 — Searle and Couette principles**

The flow profile occurring in the measuring gap of the cylinder measuring geometry is calculated according to A.3.2. The measuring gap is the space between the shell surface of the measuring bob with a radius  $R_1$  and the lateral surface of the measuring cup with a radius  $R_2$  and the same length  $L$ ; see [Figure 7](#).

#### 6.3.2.1.2 Calculation methods

Calculations of the shear stress  $\tau$  and shear rate  $\dot{\gamma}$  are ideally based on representative values that do not occur at the inner radius of the outer cylinder  $R_2$  or outer radius of the inner cylinder  $R_1$  of the measuring geometry but at a particular geometric position within the measuring gap.  $\tau_{\text{rep}}$  is defined as the arithmetic mean of the shear stresses at the outer cylinder  $\tau_1$  and inner cylinder  $\tau_2$ , which is a good approximation for the given ratio of radii ( $\delta \leq 1,1$ ). For larger values and thus for relative measuring geometries see [6.3.3.2](#).

This document confines itself solely to [Formula \(13\)](#):

$$\tau = \tau_{\text{rep}} = \frac{\tau_1 + \tau_2}{2} \quad (13)$$

where

$\tau_1$  is the shear stress at the outer radius of the inner cylinder, in pascals;

$\tau_2$  is the shear stress at the inner radius of the outer cylinder, in pascals;

[Formula \(14\)](#) applies for the representative shear stress:

$$\tau_{\text{rep}} = k_{\tau} \cdot M = \frac{1 + \delta^2}{2 \cdot \delta^2} \cdot \frac{1}{2\pi \cdot L \cdot R_1^2 \cdot c_L} \cdot M \quad (14)$$

where

$k_{\tau}$  is the shear stress factor for the conversion of torque into shear stress, in reciprocal cubic metres;

$R_1$  is the outer radius of the inner cylinder, in metres;

$\delta$  is the ratio of the inner radius of the outer cylinder and outer radius of the inner cylinder;

$L$  is the length of the inner cylinder, in metres;

$M$  is the torque, in newton multiplied by metres;

$c_L$  is the face factor, dimensionless.

The face factor depends on the measuring geometry and on the rheological properties of the sample and shall be determined experimentally.

[Formula \(15\)](#) applies to the representative shear rate,  $\dot{\gamma}_{\text{rep}}$ :

$$\dot{\gamma}_{\text{rep}} = k_{\dot{\gamma}} \cdot \Omega = \frac{1 + \delta^2}{\delta^2 - 1} \cdot \Omega = \frac{1 + \delta^2}{\delta^2 - 1} \cdot 2\pi \cdot n \quad (15)$$

where

$k_{\dot{\gamma}}$  is the shear rate factor for the conversion of angular velocity into shear rate, in reciprocal radians;

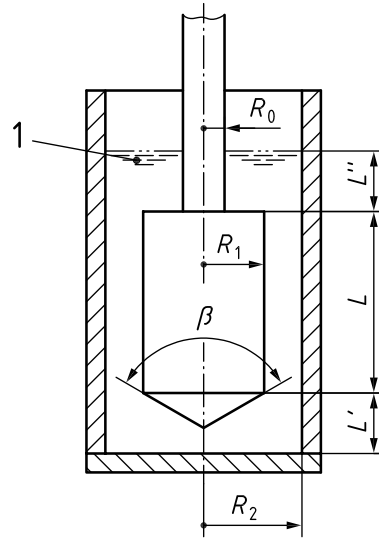
$n$  is the rotational speed, in reciprocal seconds;

$\Omega$  is the angular velocity, in radians per second.

This results in the following for a standard geometry with  $\delta = 1,084\ 7$ , given in [Formulae \(16\)](#) and [\(17\)](#):

$$\tau_{\text{rep}} = 0,044\ 6 \cdot \frac{M}{R_1^3} \quad (16)$$

$$\dot{\gamma}_{\text{rep}} = 77,46 \cdot n \quad (17)$$

**Key**

- 1 sample
- $R_0$  radius of the shaft
- $R_1$  outer radius of the inner cylinder
- $R_2$  inner radius of the outer cylinder
- $\beta$  opening angle of the face on the bottom of the inner cylinder
- $L$  length of the inner cylinder
- $L'$  distance between the lower edge of the inner cylinder and the bottom of the outer cylinder
- $L''$  immersed shaft length

**Figure 7 — Standard measuring geometry for coaxial cylinders**

For the standard measuring geometry for coaxial cylinders shown in [Figure 7](#), the face factor  $c_L$  (drag coefficient for the face surface correction that takes into account the torque acting at the end surfaces of the measuring geometry) was determined experimentally and has a value of  $c_L = 1,1$  for samples with Newtonian flow behaviour for ratios given in [Formula \(18\)](#). Deviations from 1,1 are possible and require experimental determination of the face factor.

For the standard measuring geometry for coaxial cylinders, the following ratios apply:

$$\frac{L}{R_1} = 3, \frac{L'}{R_1} = 1, \frac{L''}{R_1} = 1, \frac{R_0}{R_1} = 0,3, \delta = \frac{R_2}{R_1} = 1,0847, \beta = 120^\circ \quad (18)$$

where

$L'$  is the distance between the lower edge of the inner cylinder and the bottom of the outer cylinder, in metres;

$L''$  is the immersed shaft length, in metres;

$R_0$  is the radius of the shaft, in metres;

$R_2$  is the inner radius of the outer cylinder, in metres;

$\beta$  is the opening angle of the face on the bottom of the inner cylinder, in degrees.

### 6.3.2.1.3 Advantages and disadvantages

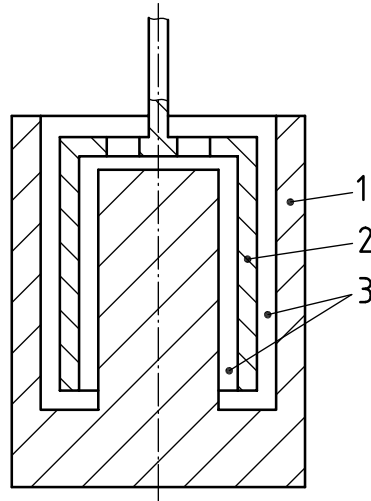
- Advantages:
  - determination of absolute measured values;
  - handling errors due to overfilling and underfilling are smaller than for cone-plate and plate-plate measuring geometries;
  - depending on the gap width, also suitable for coarsely dispersed samples (rule of thumb: gap at least 10 times larger than the diameter of the dispersed material, e.g. particles, droplets);
  - almost no evaporation influence due to small boundary surface compared to the sample volume;
  - viscosity range from low to high viscosities can be covered by varying the dimensions of the coaxial cylinders measuring geometry;
  - low distribution of shear rates in the measuring gap compared to the plate-plate measuring geometry.
- Disadvantages:
  - depending on the sensitivity of the measuring device and the measuring geometry that is used, a larger sample volume is required than with cone-plate and plate-plate measuring geometries;
  - generally higher mass inertia compared to cone-plate and plate-plate measuring geometries;
  - more laborious cleaning compared to cone-plate and plate-plate measuring geometries;
  - more severe damage to the sample structure when inserting the rotor into the sample compared to the plate-plate measuring geometry with gap setting controlled by normal force;
  - lower heating and cooling rates can be realized and therefore longer temperature control times are required due to the larger sample volume and the larger dimensions of the measuring geometry compared to cone-plate and plate-plate measuring geometries;
  - danger of air bubble entrapment when inserting the rotor into the sample.

### 6.3.2.2 Double-gap measuring geometry

#### 6.3.2.2.1 Description of the measuring geometry

The measuring geometry is a variant of a coaxial measuring geometry and consists of a measuring cup with an inner insert and a hollow cylinder that are positioned coaxially relative to one another, as shown in [Figure 8](#).

With the double-gap measuring geometry, the shear stress  $\tau$  and shear rate  $\dot{\gamma}$  in the measuring gap are not constant, but instead decrease from the inside to the outside. The calculation assumes a representative measured value within the measuring gap.

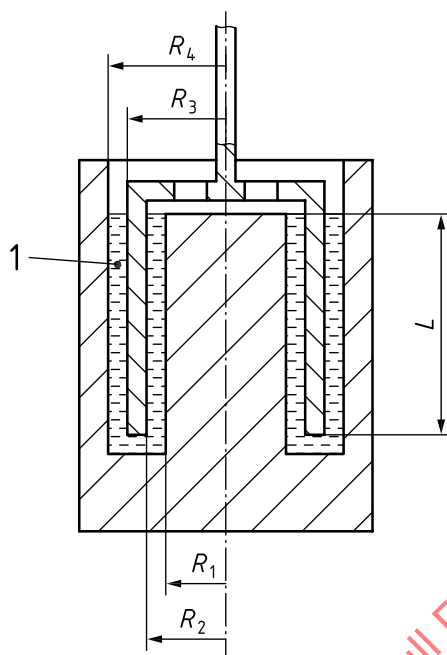
**Key**

- 1 measuring cup with inner insert
- 2 hollow cylinder with vent holes
- 3 sample chamber

**Figure 8 — Schematic drawing of a double-gap measuring geometry**

STANDARDSISO.COM : Click to view the full PDF of ISO 3219-2:2021

6.3.2.2.2 Calculation method



Key

- 1 sample
- $L$  effective length of the hollow cylinder
- $R_1$  outer radius of the inner insert
- $R_2$  inner radius of the hollow cylinder
- $R_3$  outer radius of the hollow cylinder
- $R_4$  inner radius of the measuring cup

Figure 9 — Double-gap measuring geometry

For the double-gap measuring geometry, the following ratios apply based on [Figure 9](#):

$$\delta = \frac{R_2}{R_1} = \frac{R_4}{R_3} \leq 1,15 \quad (19)$$

$$\frac{L}{R_3} \geq 3 \quad (20)$$

The following applies for the representative shear stress:

$$\tau_{\text{rep}} = \frac{1 + \delta^2}{4\pi \cdot L (\delta^2 R_3^2 + R_2^2)} \cdot M \quad (21)$$

The representative shear rate is calculated analogously to the coaxial cylinders measuring geometry:

$$\dot{\gamma}_{\text{rep}} = \frac{1 + \delta^2}{\delta^2 - 1} \cdot \Omega = \frac{1 + \delta^2}{\delta^2 - 1} \cdot 2\pi \cdot n \quad (22)$$

where

- $\delta$  is the radius ratio;
- $L$  is the effective length of the hollow cylinder, in metres;
- $R_1$  is the outer radius of the inner insert, in metres;
- $R_2$  is the inner radius of the hollow cylinder, in metres;
- $R_3$  is the outer radius of the hollow cylinder, in metres;
- $R_4$  is the inner radius of the measuring cup, in metres;
- $c_L$  is the face factor, dimensionless.

This face factor depends on the measuring geometry and on the rheological properties of the sample and shall be determined experimentally.

### 6.3.2.2.3 Advantages and disadvantages

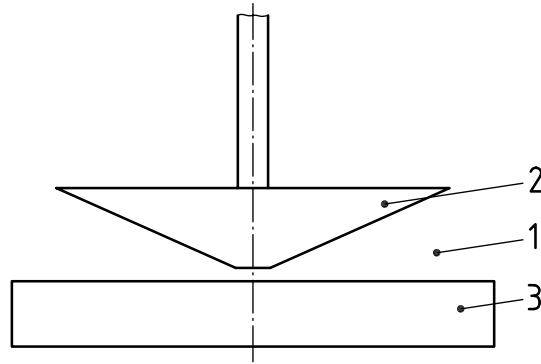
See 6.3.2.1.3. Additionally, or as deviations, the following applies.

- Advantages:
  - extension of the achievable measuring range for low-viscosity samples due to the larger measuring area compared to the coaxial cylinders measuring geometry;
  - more suitable for oscillatory measurements as the inertia moment of the double-gap measuring geometry is significantly lower than that of the cylinder measuring geometry for the same outer diameter of the measuring bob.
- Disadvantages:
  - a filling error has a greater impact compared to the coaxial cylinders measuring geometry;
  - only suitable for low-viscosity samples.

### 6.3.2.3 Cone-plate measuring geometry

#### 6.3.2.3.1 Description of the measuring geometry

The measuring geometry consists of a cone and plate (see [Figure 10](#)).



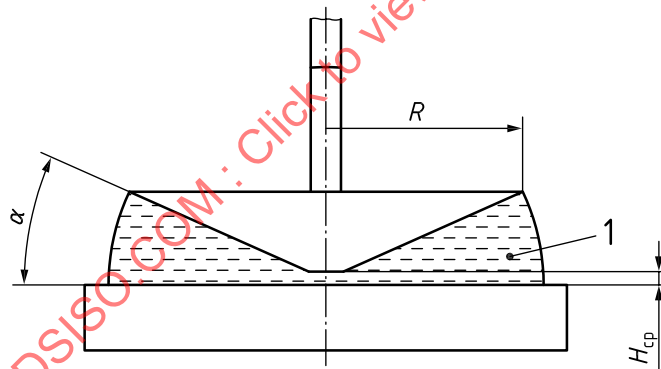
**Key**

- 1 sample chamber
- 2 cone
- 3 plate

**Figure 10 — Schematic drawing of a cone-plate measuring geometry**

The angle between the cone and the plate (cone angle) shall be as small as possible, and under no circumstances greater than 5°. The influence of friction between the cone tip and plate is avoided by the flattened cone tip (truncated cone). The flattened cone tip and angle create the specified measuring gap for the individual cone. See [Figure 11](#) for details. The extent to which the cone tip decreases, i.e. the distance between the flattened cone tip and the plate, has an impact on the measuring result.

NOTE There are also cone geometries with non-flattened cone tips.



**Key**

- 1 sample
- $R$  radius of the cone
- $\alpha$  cone angle
- $H_{cp}$  distance between flattened cone tip and plate

**Figure 11 — Cone-plate measuring geometry**

**6.3.2.3.2 Calculation method**

The derivation of shear stress or shear rate for this cone-plate measuring geometry is presented in A.3.3. For cone angles > 3°, the exact formulae in A.3.3 and [Formulae \(23\)](#) and [\(24\)](#) shall be used.

If  $\alpha \leq 0,05$  rad (i.e.  $\alpha \leq 3^\circ$ ), [Formulae \(23\)](#) and [\(24\)](#) can be used for calculating the shear stress and shear rate:

$$\tau = \frac{3M}{2\pi R^3} \quad (23)$$

where

$M$  is the torque, in newton multiplied by metres;

$R$  is the radius of the cone, in metres.

$$\dot{\gamma} = \frac{\Omega}{\alpha} \quad (24)$$

where

$\alpha$  is the angle between the cone and plate, in radians;

$\Omega$  is the angular velocity, in radians per second.

#### 6.3.2.3.3 Advantages and disadvantages

— Advantages:

- determination of absolute measured values;
- for smaller cone angles, the shear strain or shear rate in the cone gap can be considered to be sufficiently constant;
- faster cleaning compared to coaxial cylinders and double-gap measuring geometries;
- lower filling amount than with coaxial cylinders measuring geometries;
- viscosity range from low to high viscosities can be covered by varying the dimensions of the cone-plate measuring geometry;
- low inertia moment compared to coaxial cylinders measuring geometries, i.e. better detection of short-term effects, e.g. in oscillatory, creep and relaxation experiments;
- shorter temperature control times and higher heating and cooling rates compared to coaxial cylinders and double-gap measuring geometries.

— Disadvantages:

- gap width significantly smaller than with coaxial cylinders measuring geometries, which limits the maximum size of the dispersed material (e.g. particles, droplets);
- may be used in dispersed systems only if the diameter of the dispersed material (e.g. particles, droplets) is a maximum of 1/10 of the distance between flattened cone tip and plate,  $H_{cp}$  (see [Figure 11](#));
- strong influence of potential solvent evaporation due to a larger boundary surface relative to the sample volume (the use of a solvent trap minimizes the effect);
- higher impact due to underfilling and overfilling compared to coaxial cylinders and double-gap measuring geometries;
- high influence on the sample structure is possible through trimming;

- greater influence of a change of the gap width through temperature changes;
- greater influence of changes in the surface roughness, e.g. through abrasive samples or wrong cleaning procedure;
- unsuitable for sedimenting samples;
- emptying of the measuring gap is possible.

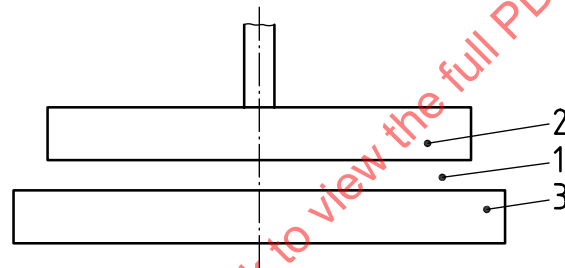
### 6.3.3 Relative measuring geometries

#### 6.3.3.1 Plate-plate measuring geometry

In contrast to the cone-plate measuring geometry, the shear rate in the measuring gap is not constant in the case of a plate-plate measuring geometry. By using corrections, it is possible to obtain identical measured values with a plate-plate measuring geometry compared to an absolute measuring geometry, see [6.3.3.1.2](#). This does not apply for all other relative measuring geometries.

##### 6.3.3.1.1 Description of the measuring geometry

The measuring geometry consists of upper and lower plates that are plane-parallel to one another (see [Figure 12](#)).



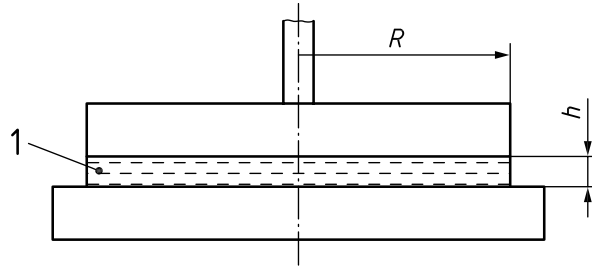
**Key**

- 1 sample chamber
- 2 upper plate
- 3 lower plate

**Figure 12 — Schematic drawing of a plate-plate measuring geometry**

The gap width  $h$  between the plates (see [Figure 13](#)) can be selected freely. One mm is a common value in practice. However, the gap width  $h$  shall be selected to ensure that the lower and upper measuring plates are fully wetted by the sample. The gap width  $h$  shall also be selected so that the dimension of any potential heterogeneity in the sample is at least 10 times smaller than the gap width  $h$ . When the gap width is being selected, the measurement errors that occur for very small and very large gap widths are to be considered.

With this measuring geometry, a radial distribution of the shear strain or shear rate results, i.e. it varies from zero at the centre of the plate to a maximum value at the edge of the plate. With a preset angular velocity, the measured torque depends directly on the flow function of the sample across the entire shear rate distribution in the measuring gap. This also applies in the case that a torque is preset and the angular velocity is measured. This is the main reason why this measuring geometry is considered to be a relative measuring geometry.

**Key**

- 1 sample  
 R radius of the plate  
 h variable gap width

**Figure 13 — Plate-plate measuring geometry**

**6.3.3.1.2 Calculation method**

For non-Newtonian liquids, the Rabinowitsch-Weissenberg correction<sup>[4]</sup> shall be performed for the calculation of the shear stress  $\tau$  and the shear rate  $\dot{\gamma}$ .

[Formulae \(25\)](#) and [\(26\)](#) can be used for these calculations solely for Newtonian liquids and, in addition, solely for the outer edge of the plate:

$$\tau = \frac{2}{\pi R^3} \cdot M \quad (25)$$

where

$M$  is the torque, in newton multiplied by metres;

$R$  is the radius of the plate, in metres.

$$\dot{\gamma} = \frac{R}{h} \cdot \Omega \quad (26)$$

where

$h$  is the variable gap width, in metres;

$\Omega$  is the angular velocity, in radians per second.

**6.3.3.1.3 Advantages and disadvantages**

See also [6.3.2.3.3](#). Additionally, or as deviations, the following applies.

— Advantages:

- variable gap width, taking into account the sample properties and the limits of the measuring device;
- different special designs and materials is possible, e.g. aluminium single-use plates, quartz glass plates, acrylic plates;
- filling method, that retains the structure of the sample, is possible with the gap setting controlled by normal force;

- measuring of coarsely dispersed samples is possible;
  - volume changes due to physico-chemical reasons in the sample can be compensated by changing the measuring gap, e.g. cross-linking shrinkage, swelling, thermal expansion of samples;
  - wall slip can be quantified by using plates with the same diameters but different surface structures, e.g. through profiling or sandblasting.
- Disadvantages compared to absolute measuring geometries: in the case of non-Newtonian samples, relative measured values are obtained if the Rabinowitsch correction is not considered.

**6.3.3.2 Coaxial relative cylinder measuring geometries with a radius ratio >1,1**

These measuring geometries are relative measuring geometries as the procedure for determining the representative values according to A.3.2 cannot be used. In this case, the determination of the values relates to the radius of the inner cylinder of the measuring geometry. In the case of non-Newtonian liquids, deviations occur relative to measuring results that were determined using the standard geometry.

**6.3.3.3 Relative measuring geometries with surface modification**

Measuring geometries of this type are used in the case of undesired sample-related effects. Wall slip and sedimentation are examples of this. A surface modification means a deviation relative to the described previously measuring geometries (plate-plate, cone-plate and coaxial cylinders measuring geometries) as a result of additional machining of the surface that is in contact with the sample. This includes profiling [e.g. vertical – see Figure 14, a)], a cylinder with a spiral groove [see Figure 14, b)], sandblasting and coating, for example. The measured values depend on the surface modification.

- Advantages:
  - prevention of undesired sample-related effects;
  - controlled generation or suppression of wall slip effects.
- Disadvantages:
  - more laborious cleaning for profiled measuring geometries;
  - restriction of the minimum gap width for profiled measuring geometries.

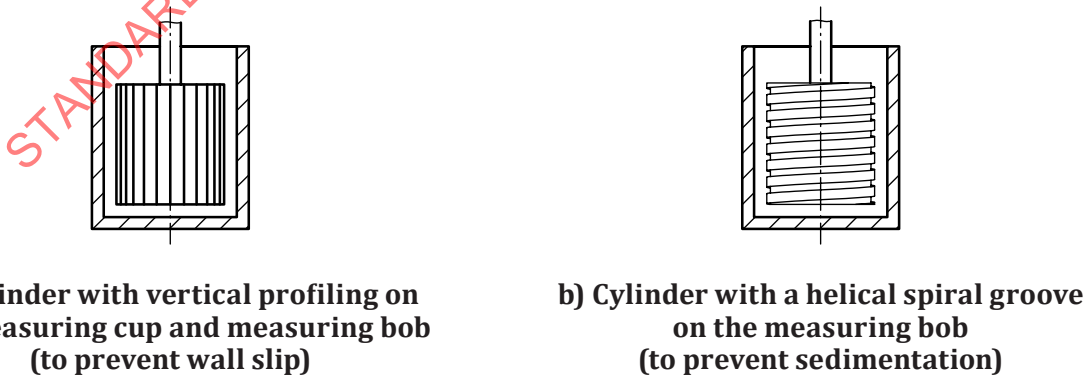


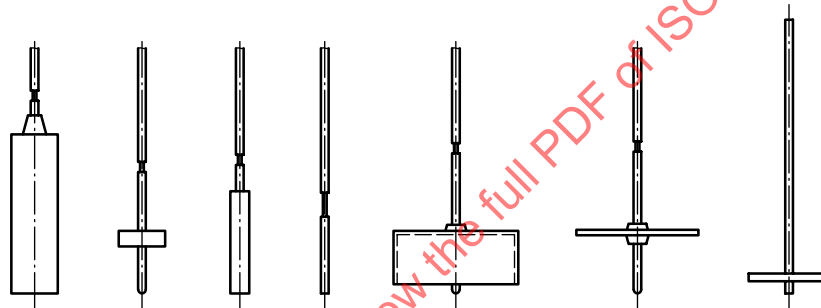
**Figure 14 — Relative measuring geometries with surface modification**

### 6.3.3.4 Selected special designs of relative measuring geometries

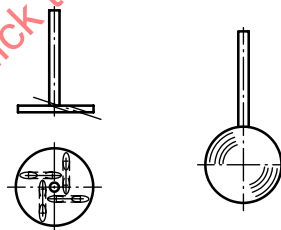
A selection of relative measuring geometries is shown in [Figure 15](#). With measuring geometries of this type, absolute measured values cannot be determined, so these measured values shall be marked in the test report as relative values. This also applies if the measurement system (measuring device and measuring geometry) was adjusted with a reference fluid (see [3.6](#)).

Relative measuring geometries are always used when absolute measuring geometries cannot be used. This applies to the following, for example:

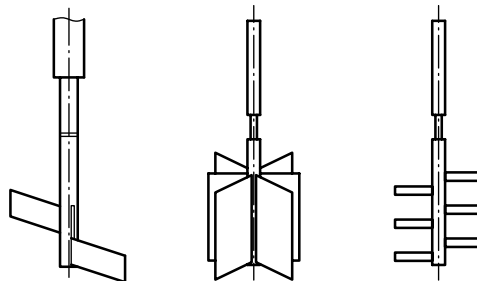
- samples with particles larger than 1/10 of the selected gap width;
- measurements in original containers;
- optimization of the test procedure to start the measurement with minimal influencing of the structure when approaching the measuring position;
- helipath test procedure, this is a vertical movement of the rotating measuring geometry during the measurement.



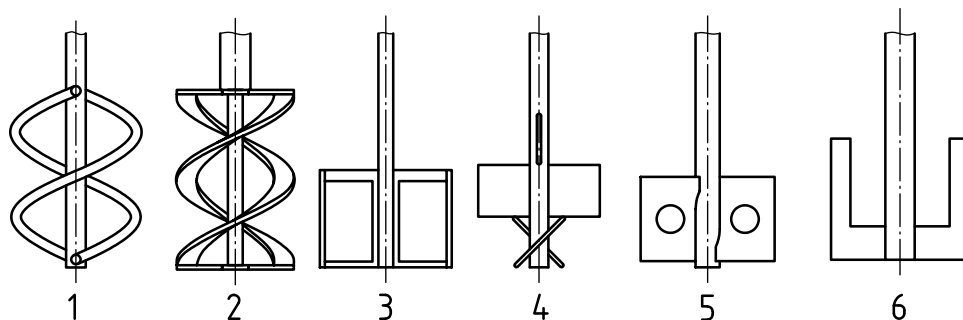
a) Examples of rotors (spindles) as per ISO 2555



b) Rotors (disc or ball spindle)



c) Rotors (paddle spindle as per ASTM D562<sup>[2]</sup>), vane rotors and pin rotors



d) Other designs for rotors

**Key**

- 1 helical shape
- 2 helical shape
- 3 blade shape
- 4 blade shape
- 5 blade shape
- 6 anchor shape

**Figure 15 — Examples of relative measuring geometries**

## — Advantages:

- extension of the area of application of the measuring device as it often represents the only possibility to carry out a measurement;
- to simulate process-dependent parameters;
- controlled generation of turbulent flow for designing process equipment.

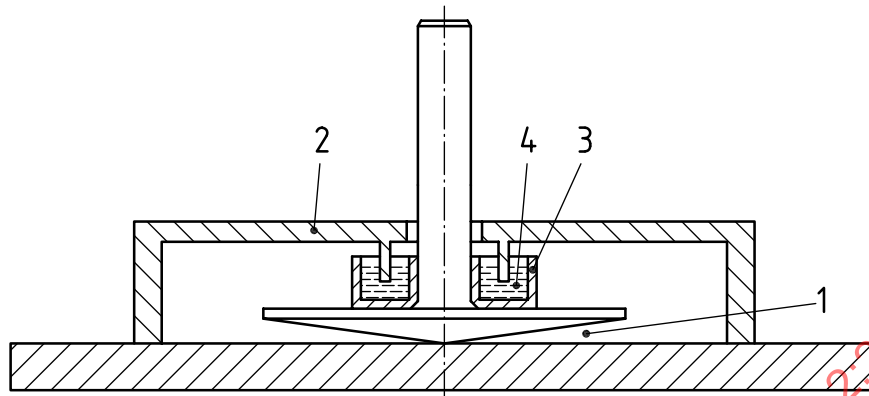
## — Disadvantages:

- no absolute measured values and thus no comparability with other measurement results that were not measured with exactly this relative measuring geometry under the same measurement conditions (e.g. rotational speed, temperature, measuring cup);
- calculation of the flow profile is not possible;
- generally requires use of larger sample volumes;
- generally difficult to control the temperature.

**6.4 Selected optional accessories****6.4.1 Cover with or without solvent trap**

After the sample has been added, a cover containing a solvent trap can be used to minimize the escape of volatile components during the measurement period (see [Figure 16](#)). The solvent trap includes half shells and a solvent reservoir in order to achieve a saturated atmosphere in the space enclosed by the cover. The half shells are positioned around the shaft of the measuring geometry; the reservoir has been previously filled with a fluid so that the half shells are immersed in the reservoir and thus create a vapour barrier. There shall not be any mechanical contact between the half shells and the shaft of the measuring geometry. On the one hand, the reservoir shall be filled sufficiently during the entire measurement period to create a vapour barrier; on the other hand, no fluid may escape from the reservoir and come into contact with the sample.

Fluids with low viscosity and low vapour pressure at the relevant measuring temperature should be selected as a filling media for the reservoir, depending on the sample, e.g. water, dodecane, mineral oil.



#### Key

- 1 sample chamber
- 2 cover
- 3 solvent reservoir
- 4 solvent

**Figure 16 — Schematic drawing of a solvent trap with the example of a cone-plate measuring geometry**

The cover can also be used without a solvent trap for protection against external influences or for connecting an inert gas in order to measure sensitive samples under a protective gas atmosphere. Depending on the measuring temperatures, sample covers made of different materials are available (e.g. polytetrafluorethene or glass).

#### — Advantages:

- minimization of evaporation-related changes in the sample;
- protection of the user against escaping sample material at high shear rates;
- protection of the sample against external influences such as draughts, dust.

#### — Disadvantages:

- exact filling of the reservoir necessary;
- wrongly selected filling media can have an effect on the measuring result;
- determination of the effect of the additional torque on the measuring result;
- more laborious measurement compared to measurements without a cover;
- depending on the design, it is impossible to observe the sample/measuring gap during the measurement;
- any existing temperature gradients in the sample can only be minimized to a limited extent compared to the use of an active thermal cover.

### 6.4.2 Passive and active thermal covers

A thermal cover is to be provided to ensure a homogeneous temperature distribution in the sample in the measuring gap.

A passive thermal cover generally consists of a heat-conducting layer on the inside and an outer insulating layer. The inner part is in contact with the temperature control system and conducts part of the heat flow into the measuring geometry.

With an active thermal cover, the sample is temperature-controlled uniformly from all sides.

- Advantages:
  - active thermal cover to achieve a constant temperature in the sample;
  - passive thermal cover to minimize the temperature gradient in the sample;
  - can be combined with a solvent trap;
  - protection of the user against escaping sample material at high shear rates;
  - protection of the sample against external influences such as draughts, dust;
  - with a connection for inert gas to allow for measurements under protective gas atmosphere.
- Disadvantages:
  - more laborious measurement compared to measurements without a cover;
  - additional heat capacity requires longer temperature control times for temperature equilibrium.

### 6.4.3 Stepped plates

Stepped measuring plates are available for cone-plate and plate-plate measuring geometries (see [Figure 17](#)). With these stepped plates, the lower part of the measuring geometry has the same diameter as the upper part. Apart from being the same diameter these two parts shall also be matched in their material and surface (e.g. sandblasted or profiled).



**Key**

- 1 sample chamber
- 2 upper plate
- 3 stepped plate

**Figure 17 — Schematic drawing of a plate-plate measuring geometry with lower stepped plate**

- Advantages:
  - avoids overfilling;
  - simplifies trimming: free-flowing material can run off, and excess material can be removed more easily at the edge for other samples;
  - stepped plate can be adapted for the upper geometry in terms of size, material and surface properties.
- Disadvantage: changed heat capacity compared to the standard design shall be taken into account for the temperature control time.

## Annex A (informative)

### Information on rheometry and flow field patterns

#### A.1 General

Further background information is presented in subsequent parts of ISO 3219, which are currently in preparation.

#### A.2 Rheological input and response parameters for rotation and oscillation

The corresponding parameters for the rotational measurement are listed in [Table A.1](#) and those for the oscillatory measurement are listed in [Table A.2](#).

**Table A.1 — Rotational measurement — Rheological input and response parameters**

Test type	Input	Response
Controlled rate (CR)	$\dot{\gamma}$	$\tau$
Controlled stress (CS)	$\tau$	$\gamma, \dot{\gamma}$
Controlled deformation (CD)	$\gamma$	$\tau$

**Table A.2 — Oscillatory measurement — Rheological input and response parameters**

Test type	Input		Response	
	Amplitude	Angular frequency or frequency	Amplitude	Phase angle
Controlled rate (CR)	$\dot{\gamma}_0$	$\omega$ or $f$	$\tau_0$	$\delta$
Controlled stress (CS)	$\tau_0$		$\gamma_0, \dot{\gamma}_0$	
Controlled deformation (CD)	$\gamma_0$		$\tau_0$	

The relationship between the raw data from the measuring device (mechanical parameters) and the calculated rheological parameters is shown in [Table A.3](#).

**Table A.3 — Comparison of raw data and calculated rheological parameters for rotation and oscillation**

Rheological parameter	Rotation	Oscillation
Shear stress	$\tau = k_\tau \cdot M$	$\tau_0 = k_\tau \cdot M_0$
Shear strain	$\gamma = k_\gamma \cdot \varphi$	$\gamma_0 = k_\gamma \cdot \varphi_0$
Shear rate	$\dot{\gamma} = k_\gamma \cdot \dot{\varphi}$	$\dot{\gamma}_0 = k_\gamma \cdot \dot{\varphi}_0$
Shear viscosity	$\eta = \frac{\tau}{\dot{\gamma}} = \frac{k_\tau \cdot M}{k_\gamma \cdot \dot{\varphi}} = k \frac{M}{\dot{\varphi}}$	$ \eta^*  = \frac{\tau_0}{\dot{\gamma}_0} = \frac{k_\tau \cdot M_0}{k_\gamma \cdot \dot{\varphi}_0} = k \frac{M_0}{\dot{\varphi}_0}$ $ \eta^*  = \sqrt{\eta'^2 + \eta''^2}$ $\eta^* = \eta' - i \cdot \eta''$ $\eta^* = \frac{1}{i\omega} G^*$
Shear modulus	$G = \frac{\tau}{\gamma}$	$ G^*  = \frac{\tau_0}{\gamma_0} = \frac{k_\tau \cdot M_0}{k_\gamma \cdot \varphi_0} = k \frac{M_0}{\varphi_0}$ $ G^*  = \sqrt{G'^2 + G''^2}$ $G^* = G' + i \cdot G''$

### A.3 Flow field patterns

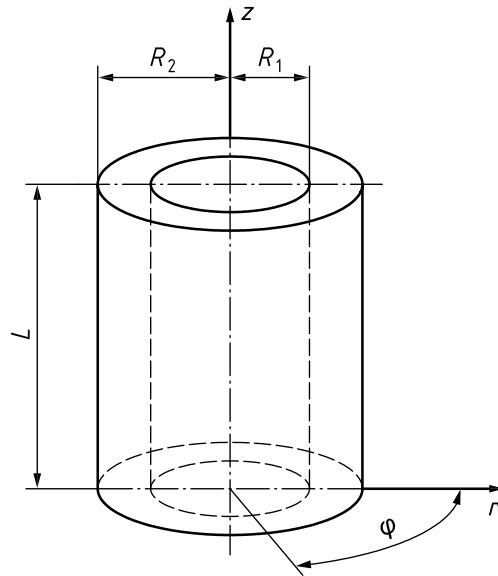
#### A.3.1 General

The flow field represents the entirety of the movement states of the sample in the measuring gap. The basic flow is the stationary flow pattern in the measuring gap at sufficiently low angular velocities  $\Omega$ . In the measuring gap of all measuring geometries, the shear stress and shear rate or shear strain are not constant and depend on the rheological properties of the sample and other factors. The mathematical calculations for absolute measurements assume that each gradient in the measuring gap is linear or can be assumed to be linear as a good approximation.

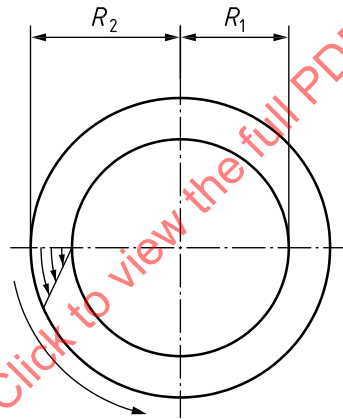
#### A.3.2 Coaxial cylinders measuring geometry

##### A.3.2.1 General

Coaxial cylinders measuring geometries with a rotating outer cylinder [Figure A.1, a)] are known as Couette measuring geometries [Figure A.1, b)], and those with a rotating inner cylinder are called Searle measuring geometries [Figure A.1, c)]. They differ in terms of the stability of their basic flow with respect to inertial forces. If not indicated otherwise, the Searle principle is assumed below.

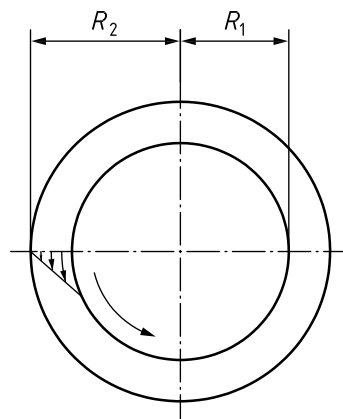


a) Cylindrical coordinates and relevant dimensions



NOTE The arrow lengths shown are proportional to the angular velocity across the measuring gap  $\omega(r)$  for Couette type.

b) Velocity profile and cross-section through the measuring gap perpendicular to the axis of rotation for Couette type



NOTE The arrow lengths shown are proportional to the angular velocity across the measuring gap  $\omega(r)$  for Searle type.

c) Velocity profile and cross-section through the measuring gap perpendicular to the axis of rotation for Searle type

**Key**

- $R_1$  outer radius of the inner cylinder
- $R_2$  inner radius of the outer cylinder
- $L$  length of the inner cylinder
- $\Phi$  angular coordinate in the cylindrical coordinate system
- $r$  radial coordinate in the cylindrical coordinate system
- $z$  axial coordinate in the cylindrical coordinate system

**Figure A.1 — Flow field patterns for basic flow in a coaxial cylinders measuring geometry**

**A.3.2.2 Description of the flow field**

Surfaces with the same angular velocity are cylinder shell surfaces for which  $r = \text{constant}$ . The boundary surfaces are characterized by  $R_1$  (outer radius of the inner cylinder) and  $R_2$  (inner radius of the outer cylinder) — see [Figure A.1](#). The radius ratio  $\delta$  and the gap width  $H_{cc}$  are defined by [Formulae \(A.1\)](#) and [\(A.2\)](#):

$$\delta = \frac{R_2}{R_1} \tag{A.1}$$

$$H_{cc} = R_2 - R_1 \tag{A.2}$$

The flow field is described using cylindrical coordinates  $r, \varphi, z$  (see [Figure A.1](#)). The flow field coefficient for a finite portion of length  $L$  of a cylinder extending infinitely in the  $z$ -direction is given by [Formula \(A.3\)](#) according to Margules<sup>[3]</sup>:

$$k = \frac{1}{4\pi \cdot L} \cdot \frac{R_2^2 - R_1^2}{R_2^2 \cdot R_1^2} = \frac{1}{4\pi \cdot L \cdot R_1^2} \cdot \frac{\delta^2 - 1}{\delta^2} \tag{A.3}$$

**A.3.2.3 Description of the basic flow**

[Formulae \(A.4\)](#) to [\(A.6\)](#) apply for the radial profile of the shear stress  $\tau$  as a function of the radius  $r$  ( $R_1 \leq r \leq R_2$ ):

$$\tau(r) = \frac{1}{2\pi \cdot L \cdot r^2} \cdot M = k_\tau \cdot M \tag{A.4}$$

$$\tau_1 = \frac{M}{2\pi \cdot L \cdot R_1^2} \tag{A.5}$$

$$\tau_2 = \frac{\tau_1}{\delta^2} \tag{A.6}$$

where  $k_\tau$  is the shear stress factor for the conversion of torque into shear stress, in reciprocal cubic metres.

In coaxial cylinders measuring geometries, surfaces with the same angular velocity are also surfaces with the same shear rate and the same shear stress. The shear rate  $\dot{\gamma}$  as a function of the radius  $r$  ( $R_1 \leq r \leq R_2$ ) is given by [Formulae \(A.7\)](#) to [\(A.9\)](#):

$$\dot{\gamma}(r) = \frac{R_1^2}{r^2} \cdot \frac{2 \cdot \delta^2}{\delta^2 - 1} \cdot \Omega = k_\dot{\gamma} \cdot \Omega \tag{A.7}$$

$$\dot{\gamma}_2 = \frac{2 \cdot \Omega}{\delta^2 - 1} \quad (\text{A.8})$$

$$\dot{\gamma}_1 = \dot{\gamma}_2 \cdot \delta^2 \quad (\text{A.9})$$

where  $k_{\dot{\gamma}}$  is the shear rate factor for the conversion of angular velocity into shear rate, in reciprocal radians.

The shear rate at the outer cylinder  $\dot{\gamma}_2$  is less than the shear rate at the inner cylinder  $\dot{\gamma}_1$ .

The radial profile of the angular velocity  $\omega(r)$  in the measuring gap differs for the Couette and Searle types, as shown below in [Formulae \(A.10\)](#) and [\(A.11\)](#):

$$\omega(r)_{\text{Couette}} = \Omega_2 \frac{\delta^2 \cdot (r^2 - R_1^2)}{(\delta^2 - 1) \cdot r^2} \quad (\text{A.10})$$

$$\omega(r)_{\text{Searle}} = \Omega_1 \frac{\delta^2 \cdot (R_2^2 - r^2)}{(\delta^2 - 1) \cdot r^2} \quad (\text{A.11})$$

where  $\omega(r)$  is the angular velocity, a variable that takes on values between  $0 < \omega(r) < \Omega_1$  for Couette types or  $0 < \omega(r) < \Omega_2$  for Searle types.

NOTE According to [Formulae \(A.4\)](#) to [\(A.9\)](#), the shear rate  $\dot{\gamma}$  and the shear stress  $\tau$  vary less at a given angular velocity  $\Omega$  in the measuring gap the narrower this gap is. If a coaxial cylinders measuring geometry apart from the standard geometry is used, the influences of a gap width that is too large are not to be neglected.

#### A.3.2.4 Standard geometry for coaxial cylinders

The cylinder geometry described does not take into account the influence of the upper and lower end faces of the measuring geometry.

With the standard geometry (see [Figure 7](#)), all the dimensions except the opening angle of the face  $\beta$  at the bottom of the inner cylinder are determined solely by geometrical ratios (relative to  $R_1$ ), which ensures that the flow field is geometrically similar regardless of the size of the measuring geometry.

The following specifications given in [Formulae \(A.12\)](#) to [\(A.14\)](#) apply:

$$\frac{L}{R_1} \geq 3, \frac{L'}{R_1} \geq 1, \frac{L''}{R_1} \geq 1, \frac{R_0}{R_1} \geq 0,3, \delta = \frac{R_2}{R_1} = 1,0847 \quad (\text{A.12})$$

NOTE The numerical value  $\delta = 1,0847$  is based on the specification in [Formula \(A.13\)](#).

$$\left( \frac{R_1}{R_2} \right)^2 = 0,85 \quad (\text{A.13})$$

$$\beta = 120^\circ \pm 1^\circ \quad (\text{A.14})$$

If these specifications are adhered to, the amount (filling volume) of sample required is given by [Formula \(A.15\)](#):

$$V = 8,17 \cdot R_1^3 \quad (\text{A.15})$$

**A.3.2.5 Calculation of the coaxial cylinders measuring geometry using the method of representative viscosity**

With coaxial cylinders measuring geometries,  $\tau$  and  $\dot{\gamma}$  are not constant in the measuring gap.

Calculations of  $\tau$  and  $\dot{\gamma}$  are ideally based on representative values that do not occur at the outer radius  $R_2$  or inner radius  $R_1$  of the measuring geometry but at a particular geometric position within the measuring gap.  $\tau_{rep}$  is defined as the arithmetic mean of the shear stresses at the outer and inner cylinders, which is a good approximation for the given ratio of radii ( $\delta \leq 1,1$ ).

This document confines itself solely to the approximation given in [Formulae \(A.16\)](#) to [\(A.18\)](#):

$$\tau = \tau_{rep} = \frac{\tau_1 + \tau_2}{2} \tag{A.16}$$

or,

$$\tau = \frac{1 + \delta^2}{2\delta^2} \tau_1 = \frac{1 + \delta^2}{2} \tau_2 \tag{A.17}$$

thus,

$$\tau = \frac{1 + \delta^2}{2\delta^2} \cdot \frac{1}{2\pi \cdot L \cdot R_1^2 \cdot c_L} \cdot M \tag{A.18}$$

since the shear stresses are calculated from the torque measured at the inner or outer cylinders according to [Formula \(A.19\)](#):

$$\tau_1 = \frac{M}{2\pi \cdot L \cdot R_1^2 \cdot c_L} \text{ or } \tau_2 = \frac{M}{2\pi \cdot L \cdot R_2^2 \cdot c_L} \tag{A.19}$$

For the described standard geometry, the face factor takes on the value of  $c_L = 1,1$  for Newtonian liquids if the recommended length ratios are adhered to. The validity of this has been confirmed experimentally.

For measurement systems where the dimensions  $L^*$ ,  $\delta^*$  deviate from the preferred values  $L$ ,  $\delta$ , the  $c_L$  value can be corrected.

$$c_L^* = 1 + \frac{L}{L^*} (c_L - 1) \tag{A.20}$$

$$c_L^* = c_L + 1,04 (\delta^* - \delta) \tag{A.21}$$

The  $c_L$  value is also used as an approximation for non-Newtonian liquids.

The representative shear rate  $\dot{\gamma}_{rep}$  corresponding to the representative shear stress  $\tau_{rep}$  can be calculated using [Formulae \(A.22\)](#) and [\(A.23\)](#):

$$\dot{\gamma} = \dot{\gamma}_{rep} = \Omega \frac{1 + \delta^2}{\delta^2 - 1} \tag{A.22}$$

with

$$\Omega = 2\pi \cdot n \tag{A.23}$$

where

$\Omega$  is the angular velocity;

$n$  is the rotational speed.

If  $n$  is specified in  $s^{-1}$  and  $\Omega$  in  $rad \cdot s^{-1}$ , the numerical formula given in [Formula \(A.24\)](#) applies<sup>1)</sup>:

$$\Omega = 6,283\,2 \cdot n \quad (A.24)$$

When the standard geometry is used, the numerical formulae given in [Formulae \(A.25\)](#) to [\(A.28\)](#) apply for the evaluation:

$$\delta^2 = 1,176\,57 \quad (A.25)$$

$$\tau = \tau_{rep} = 0,925 \cdot \tau_1 = 1,088 \cdot \tau_2 \quad (A.26)$$

The following relationships apply for  $\tau$  in Pa,  $M$  in  $N \cdot m$ ,  $\dot{\gamma}$  in  $s^{-1}$  and  $\Omega$  in  $rad \cdot s^{-1}$ ,  $R_1$  in m and  $n$  in  $s^{-1}$ :

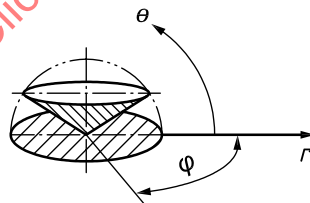
$$\tau = \tau_{rep} = 0,0446 \cdot \frac{M}{R_1^3} \quad (A.27)$$

$$\dot{\gamma} = \dot{\gamma}_{rep} = 12,33 \cdot \Omega = 77,46 \cdot n \quad (A.28)$$

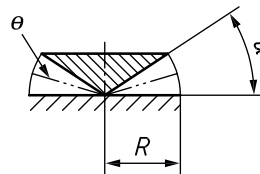
### A.3.3 Cone-plate measuring geometry

#### A.3.3.1 General

The flow field is described using spherical coordinates  $r$ ,  $\varphi$ ,  $\theta$  (see [Figure A.2](#)). The fluid is retained in the measuring gap by surface tension forces and, in the case of viscoelastic samples, also by normal forces.

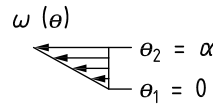


a) Spherical coordinates



b) Vertical section through measuring gap

1) The rotational speed in reciprocal seconds is used in this example. If it is expressed in reciprocal minutes, the numerical value changes accordingly.



**c) Velocity profile along the polar angle when the cone is rotating**

**Key**

- $\theta$  polar angle in the spherical coordinate system
- $\varphi$  azimuthal angle in the spherical coordinate system
- $r$  radial coordinate in the spherical coordinate system
- $\alpha$  cone angle
- $R$  radius of the cone
- $\omega$  angular velocity

NOTE For illustrative purposes, the cone angle  $\alpha$  shown is greater than that used in practice.

**Figure A.2 — Flow field for flow in a cone-plate geometry**

**A.3.3.2 Description of the flow field**

Surfaces with the same angular velocity are lateral conical surfaces for which  $\theta = \text{constant}$ . One boundary surface (the plate) with  $\theta_1$  and the cone angle  $\alpha$  are defined by [Formulae \(A.29\)](#) and [\(A.30\)](#):

$$\theta_1 = 0 \tag{A.29}$$

$$\theta_2 - \theta_1 = \alpha \tag{A.30}$$

For a finite plate radius  $R$  and a sufficiently small cone angle ( $\alpha \leq 0,05$  rad, i.e.  $\alpha \leq 3^\circ$ ), the flow field coefficient is given to a good approximation by [Formulae \(A.31\)](#) and [\(A.32\)](#):

$$k = \frac{3 \cdot \alpha \cdot f(\alpha)}{2\pi \cdot R^3} \approx \frac{3 \cdot \alpha}{2\pi \cdot R^3} \tag{A.31}$$

where, in [Formula \(A.31\)](#),

$$f(\alpha) = \frac{1}{2 \cdot \alpha} \left[ \frac{\tan \alpha}{\cos \alpha} + \frac{1}{2} \cdot \ln \left( \frac{1 + \sin \alpha}{1 - \sin \alpha} \right) \right] \tag{A.32}$$

with  $\lim_{\alpha \rightarrow 0} f(\alpha) = 1$ .

NOTE  $f(\alpha) = 1,000\ 6$  applies for  $\alpha = 2^\circ$ .  $f(\alpha) = 1,003\ 8$  applies for  $\alpha = 5^\circ$ .

**A.3.3.3 Description of the basic flow**

In cone-plate measuring geometries, surfaces with the same angular velocity are also surfaces with the same shear rate and the same shear stress. The shear rate  $\dot{\gamma}(\theta)$  and the related shear stress  $\tau(\theta)$  vary only to a small extent across the entire measuring gap of a cone-plate measuring geometry if  $\alpha \leq 0,05$  rad (i.e.  $\alpha \leq 3^\circ$ ). [Formulae \(A.33\)](#) and [\(A.34\)](#) apply:

$$\dot{\gamma}(\theta) = \frac{\Omega}{\alpha \cdot f(\alpha) \cdot \cos^2 \theta} \approx \frac{\Omega}{\alpha} \tag{A.33}$$

$$\tau(\theta) = \frac{3 \cdot M}{2\pi \cdot R^3 \cdot \cos^2 \theta} \approx \frac{3 \cdot M}{2\pi \cdot R^3} \quad (\text{A.34})$$

[Formula \(A.35\)](#) applies for the profile of the angular velocity  $\omega(\theta)$  if the cone is driven:

$$\omega(\theta) = \Omega \cdot \frac{\theta \cdot f(\theta)}{\alpha \cdot f(\alpha)} \approx \Omega \cdot \frac{\theta}{\alpha} \quad (\text{A.35})$$

and [Formula \(A.36\)](#) applies if the plate is driven:

$$\omega(\theta) = \Omega \cdot \left[ 1 - \frac{\theta \cdot f(\theta)}{\alpha \cdot f(\alpha)} \right] \approx \Omega \cdot \left[ 1 - \frac{\theta}{\alpha} \right] \quad (\text{A.36})$$

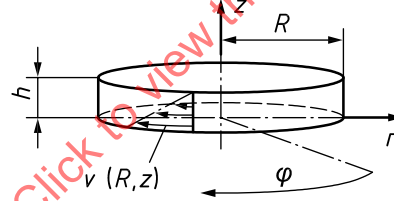
The angular velocity profile is shown in [Figure A.2, c\)](#).

### A.3.4 Plate-plate measuring geometry

#### A.3.4.1 General

When relative measuring geometries are used, the flow field coefficient is determined with a Newtonian liquid in practice, but this flow field coefficient is dependent on rotational speed and cannot be used for non-Newtonian liquids.

In contrast to the cone-plate measuring geometry, the shear rate in the measuring gap is not constant in the case of the plate-plate measuring geometry.



#### Key

- $h$  variable gap width
- $z$  axial coordinate in the cylindrical coordinate system
- $R$  radius of the plate
- $r$  radial coordinate in the cylindrical coordinate system
- $v$  circumferential angular velocity
- $\varphi$  angular coordinate in the cylindrical coordinate system

**Figure A.3 — Flow field for flow in a plate-plate geometry**

#### A.3.4.2 Description of the flow field

The flow field is described using cylindrical coordinates  $r, \varphi, z$  (see [Figure A.3](#)). Surfaces with the same angular velocity are flat circular surfaces for which  $z = \text{constant}$  perpendicular to the axis of rotation. The gap width  $h$  is the distance between the two plates.

The flow field coefficient  $k$  is calculated from the plate radius  $R$  and the gap width  $h$  according to [Formula \(A.37\)](#):

$$k = \frac{2 \cdot h}{\pi \cdot R^4} \quad (\text{A.37})$$

This relationship applies for any gap width  $h$ , but only for Newtonian liquids.

**A.3.4.3 Description of the basic flow**

With plate-plate measuring geometries, the surfaces with the same angular velocity are not surfaces with the same shear rate. In contrast, the surfaces with the same shear rate and the same shear stress are lateral cylinder surfaces for which  $r = \text{constant}$  ( $0 \leq r \leq R$ ). The shear rate  $\dot{\gamma}(r)$  as a function of the coordinate  $r$  is given by [Formulae \(A.38\)](#) and [\(A.39\)](#):

$$\dot{\gamma}(r) = \frac{\Omega}{h} \cdot r \tag{A.38}$$

$$\dot{\gamma}_{\text{max}} = \frac{\Omega}{h} \cdot R \tag{A.39}$$

[Formula \(A.40\)](#) applies for the profile of the angular velocity  $\omega(z)$  across the measuring gap:

$$\omega(z) = \frac{\Omega}{h} \cdot z \tag{A.40}$$

where  $z = 0$  at the stationary boundary surface.

The distribution of the shear rate in the measuring gap is independent of the flow properties of the sample to be examined, while the distribution of the shear stress depends on the flow properties.

For the boundary surface ( $r = R$ ) of the plate-plate geometry, [Formula \(A.41\)](#) applies:

$$\tau(R) = \frac{M}{2\pi \cdot R^3} \left( 3 + \frac{d \ln M}{d \ln \dot{\gamma}(R)} \right) \tag{A.41}$$

To calculate the shear stress for an unknown sample, a number of measurements at different angular velocities are therefore necessary to determine the gradient  $d \ln M / d \ln \dot{\gamma}(R)$ .

$d \ln M / d \ln \dot{\gamma}(R) = 1$  for Newtonian liquids, so [Formula \(A.42\)](#) applies:

$$\tau(R) = \frac{2 \cdot M}{\pi \cdot R^3} \tag{A.42}$$

**A.4 Oscillatory rheometry**

**A.4.1 General**

[Clause A.4](#) specifies the determination of the viscous and elastic behaviour of materials using oscillatory measurements. In this regard, the recording of a single measurement point is looked at first. The material behaviour is then described using several measurement points.

The following is assumed for recording a measurement point:

- the sample is deformed sinusoidally (i.e. harmonically) at constant frequency and amplitude in an oscillatory rheometer;
- the response of the sample at steady-state conditions is also harmonic at the same frequency;
- the properties of the sample do not change during the recording of the measurement points, i.e. all environmental conditions such as temperature are constant;
- the measuring gap is correctly filled during the recording of the measurement point.

Here, the frequency  $f$  or angular frequency  $\omega = 2\pi f$  is another specified parameter compared to rotational rheometry. For this reason, there is another sample response variable, the drive phase angle  $\zeta$  or the phase angle  $\delta$ . In [Table A.4](#), the mechanical and rheological parameters as functions of